

# Bi-universality characterizes a realistic spatial network model

Bnaya Gross,<sup>1</sup> Michael M. Danziger,<sup>1</sup> Sergey V. Buldyrev,<sup>2</sup> and Shlomo Havlin<sup>1,3</sup>

<sup>1</sup>*Department of Physics, Bar Ilan University, Ramat Gan, Israel*

<sup>2</sup>*Department of Physics, Yeshiva University, New York, New York 10033, USA*

<sup>3</sup>*Institute of Innovative Research, Tokyo Institute of Technology, Midori-ku, Yokohama, Japan 226-8503*

(Dated: April 4, 2017)

One of the most powerful findings of statistical physics is the discovery of *universality classes* which can be used to categorize and predict the behavior of seemingly different systems. However, many real-world complex networks have not been fitted to the existing universality classes. Here, we study a realistic spatial network model with link-lengths of a characteristic scale  $\zeta$ . We find that this simple spatial network topology, though not fulfilling the requirements of any single universality class, exhibits a new *multiple universality* composed of two sets of critical exponents at a *unique critical threshold*. This bi-universality is characterized by mean-field scaling laws for measurements on a scale smaller than  $\zeta$  but spatial scaling for measurements on a larger scale. We verify this multiple universality by measuring the percolation critical exponents  $\nu$  (correlation length),  $\beta$  (giant component),  $\gamma$  (mean mass) as well as scaling relations for chemical vs geometric distance and epidemic dynamics. By introducing the concept of multiple universality we are able to generalize the concept of universality for complex topologies.

Critical phenomena on networks can be simplified by determining their universality class. As soon as the universality class is known, the scaling behavior for many processes can be predicted [1–5]. The universality class of a particular system is determined by the dimension of the space where the system is embedded, and the type of the interactions among their constituents. Once the critical exponents of a specific system have been determined, then they will be the same for all other systems in the same class. Well-studied universality classes contain the Ising model [1, 6, 7], polymers [8], mean field theory [1, 2] and percolation on lattices [5, 9–12].

The scaling relations at criticality observed in percolation include the size of the giant component, the correlation length and the average size of finite clusters. These scaling exponents are related to each other by means of a set of scaling relations [3], which show that only two of them (e.g.  $\beta$  and  $\nu$ ) are actually independent.

Here we show that realistic models for spatial networks with finite characteristic link length  $\zeta$  are bi-universal. By bi-universality, we mean that they are characterized simultaneously at a unique critical threshold by two sets of critical exponents. The scaling behavior follows the universality class of random networks for short scales measurements (below  $\zeta$ ) and the class of spatial networks for long scale measurements (above  $\zeta$ ). Networks of finite characteristic length are ubiquitous in infrastructure [13, 14], the brain [15, 16] and other systems [17, 18].

Complex networks are typically studied as either spatial or random [17–20]. Specific examples include, the well-known small-world model [21, 22], the parametrized cost models [4, 23], and the random networks ranging from Erdős-Rényi to the scale free model [24].

Here we systematically study the universality class of a recently developed spatial network model (SNM), whose aim is to give a better description of real-world spacial networks and their resilience [13, 25]. In this model each node of the lattice (network) interacts on average with  $k$

other nodes within some finite geometric distance  $\zeta$ . The construction of the network follows three stages: (i) randomly choose a source node in the lattice, (ii) generate a link-length  $r$  from the distribution

$$P(r) \sim \exp(-r/\zeta), \quad (1)$$

(iii) randomly choose a target node with a distance to the source closest to  $r$  and connect them if they are not already connected. Repeat this process until achieving the average degree  $k$  which is a parameter of the model. Similar models have been studied but the universality features have not been explored [26–28].

Here we consider a network with  $k = 4$ , as in a square lattice. We begin by removing a fraction  $1 - p$  of nodes (site percolation) and measure the correlation length of the network,  $\xi$ , close to criticality as a function of  $|p - p_c|$ , for a unique critical threshold  $p_c$ , for which we use a new algorithm [29] to analyze large networks ( $N \sim 10^8$ ).

As can be seen in Fig. 1, there are two regions with different slopes representing two values for  $\nu$ , the critical exponent of  $\xi$ . For large values of  $\xi$ , very close to criticality,  $\xi$  scales with  $\nu \approx 4/3$ , while for small values, it scales with  $\nu \approx 0.5$ . As  $\zeta$  increases the crossover between the two critical exponents occur closer to criticality. The lower inset of Fig. 1 shows the unique critical threshold.

To understand the origin of the two regions of critical exponents we note that for short range ( $r < \zeta$ ) the structure of the lattice is not relevant since every pair of nodes can be connected with almost the same probability, Eq. (1). This results in a mean field behavior because the space becomes irrelevant, similar to  $d \geq 6$  [5, 10]. However, for longer range ( $r > \zeta$ ) the structure of the lattice determines the behavior since the link-lengths are much shorter than the measurement scale.

This explains the behavior seen in Fig. 1 since the values of the critical exponent  $\nu$  are known to be  $\nu_{\text{lattice}} = 4/3$  and  $\nu_{MF} = 0.5$  for lattice and mean field respectively [5]. Thus, at large scales,  $\xi$  follows the scaling behavior

of spatial networks and therefore, the critical exponent  $\nu$  takes the value of  $4/3$ , and at short scales  $\xi$  follows the scaling behavior of a random network and thus  $\nu$  obtains the value of  $0.5$ . Generally, we find that  $\xi$  follows the relation:

$$\xi \sim |p - p_c|^{-\nu} \quad \text{where} \quad \begin{cases} \nu = 1/2 & p > p^* \\ \nu = 4/3 & p_c < p < p^* \end{cases} \quad (2)$$

with two different exponents when  $p$  approaches the unique critical threshold,  $p_c$ . Indeed, as  $\zeta$  increases, the region that follows mean field behavior becomes larger and the crossover occur closer to criticality.

We can evaluate the crossover point,  $p^*$ , at which the critical exponent changes. At  $p^*$  we expect that  $\xi$  is the same for mean field and lattice. Therefore,  $\xi \sim |p^* - p_c|^{-4/3} \sim |p^* - p_c|^{-1/2}\zeta$ , where  $\zeta$  is the scale of the mean field region. Thus, we obtain the relation:

$$(p^* - p_c) \sim \zeta^{-6/5} \quad (3)$$

for the crossover point, which we verify in the top inset of Fig. 1. We hypothesizes that the two regions with different scaling found for  $\xi$  in Eq. (2) appear in every scaling property which can be measured at short range (where we expect MF) and long range (where we expect spatial). We validate this hypotheses below for several other measurements.

Next we test the bi-universality hypothesis in the relative size of the giant connected component,  $P_\infty$ , near criticality. In percolation theory,  $P_\infty = 0$  for  $p < p_c$  and  $P_\infty \sim (p - p_c)^\beta$  above and near  $p_c$ . In Fig. 2(a), the two critical exponents for  $\beta$  are shown to coexist in the same system. At large scales, close to criticality, the giant size demonstrate scaling behavior with  $\beta \approx 5/36$  while at short scales the scaling behavior has  $\beta \approx 1$ . Again, as  $\zeta$  increases the crossover between the two critical exponents emerges at larger scales, i.e., closer to criticality. Indeed, the values of the critical exponent  $\beta$  have already been calculated for lattice and mean field respectively to be  $\beta_{lattice} = 5/36$  and  $\beta_{MF} = 1$  [5, 10]. Thus, at large scales,  $P_\infty$  follows scaling behavior of  $2d$  spatial networks, and at short scales  $P_\infty$  follows scaling behavior of a random network. Generally, we suggest that  $P_\infty$  follows the relation:

$$P_\infty \sim (p - p_c)^\beta \quad \text{where} \quad \begin{cases} \beta = 1 & p > p^* \\ \beta = 5/36 & p_c < p < p^* \end{cases} \quad (4)$$

when  $p$  approaches  $p_c$ . This relation is valid only above and near criticality since below criticality the giant component does not exist and  $P_\infty = 0$ .

The critical behavior of the mean mass of all the finite clusters near criticality, also shows the analogous bi-universality phenomena. For details see the supplementary information.

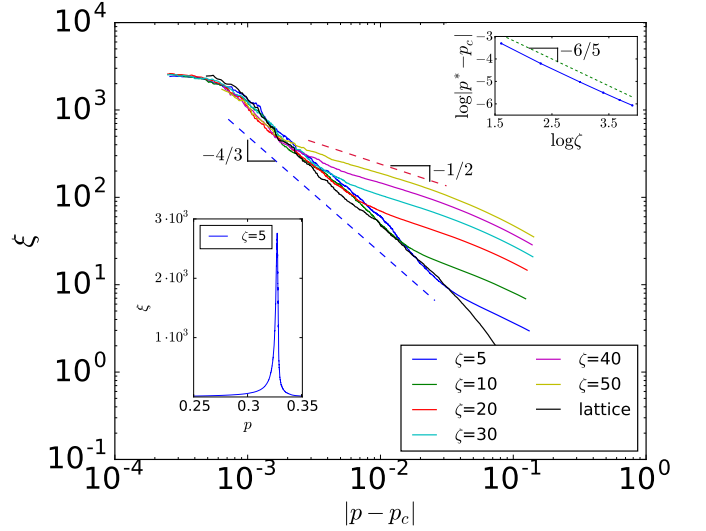


FIG. 1: **The percolation correlation length  $\xi$  as a function of  $|p - p_c|$  above criticality ( $p > p_c$ ).** It is seen that two critical exponents coexist,  $\nu_{lattice} = 4/3$  appears for large distances (large  $\xi$  i.e., small  $|p - p_c|$ ) and  $\nu_{MF} = 0.5$  appears for short distances (small  $\xi$  i.e., relatively large  $|p - p_c|$ ). As  $\zeta$  increases the crossover emerges closer to criticality as expected. The lower inset shows the divergence of  $\xi$  at  $p_c$  for  $\zeta = 5$ . The top inset shows the scale of the crossover point,  $p^*$  with  $\zeta$  which follow the relation:  $(p^* - p_c) \sim \zeta^{-6/5}$ , see Eq. (3). The values of  $p_c$ , monotonically decrease with  $\zeta$  from  $p_c = 1/\langle k \rangle = 0.25$  for  $\zeta \rightarrow \infty$ , to  $p_c \approx 0.5927$ , for  $\zeta \rightarrow 0$ , for which we recover the value known for site percolation on the square lattice [5, 10]. Simulations shown for  $N = 10^8$ , average over 200 realizations.

While the quantities studied before were near criticality, we show now the bi-universality for quantities measured exactly at criticality. To this end we analyze the geometric distance as a function of chemical distance between pairs of nodes on the giant component *at criticality* [5]. We denote by  $\langle r \rangle$  the average geometric distance at a chemical distance  $l$  which is the minimal number of hops between them.

The algorithm to measure this quantity is as follow: (i) randomly select a single node in the giant component to be a source node, (ii) measure the geometric distances from this source to all nodes at  $l$  steps away from the source, (iii) average all the geometric distances obtained in step (ii). Repeat this process over all the nodes in the giant component, and average over all sources. We found above that our network behaves for scales smaller than  $\zeta$  as mean field and above  $\zeta$  as a lattice. Thus, we expect that the behavior of the network will follow:

$$\langle r \rangle = \begin{cases} l^{1/2} & l \leq l^* \quad (MF) \\ l^{1/d_{min}} & l > l^* \quad (lattice) \end{cases} \quad (5)$$

These two exponents  $1/2$  and  $1/d_{min}$  are expected since they have been found for percolation in  $d \geq 6$  (MF) and

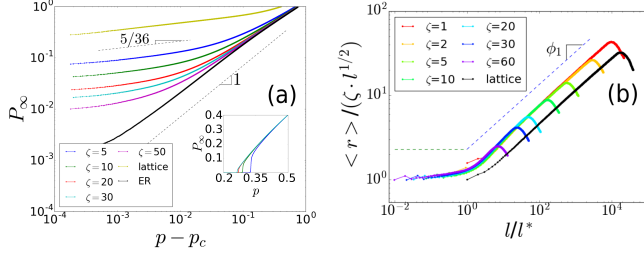


FIG. 2: **(a) The giant component,  $P_\infty$ , as a function of  $p - p_c$  above criticality.** We see the coexistence of two critical exponents:  $\beta_{lattice} = 5/36$  for large distances (small  $p - p_c$ ) and  $\beta_{MF} = 1$  for short distances (large  $p - p_c$ ). The crossover emerges closer to  $p_c$  as  $\zeta$  increases. The inset shows the behavior of  $P_\infty$  vs  $p$  in linear scales for several values of  $\zeta$  (5, 10, 20, 30 from right to left). **(b) The average geometric distance  $\langle r \rangle$  as a function of the chemical distance  $l$  at criticality.** Both y-axis and x-axis are scaled according to Eq. (6). The scaling relation is:  $r = \zeta l^{1/2} f(\frac{l}{l^*})$  where  $l^* = \zeta^{d_{min}}$ . It can be seen that after the scaling, the graph starts as nearly constant behavior for  $\frac{l}{l^*} \ll 1$  and then crosses over at  $l \sim l^*$  to a slope with exponent  $\phi_1$  as suggested by Eq. (7). Note that for the pure lattice the constant region does not exist and as  $\zeta$  increases the constant region gets longer while the region with the exponent  $\phi_1$  gets shorter. The bending down of the curves is due to the finite size of the systems. For infinite systems the bending down is expected to disappear. Simulations shown for  $N = 10^8$ , average over 200 realizations.

for  $d = 2$  respectively [5]. Note that in contrast to the other exponents (e.g.,  $\beta$  and  $\nu$ ) the value  $d_{min} \approx 1.13$  is not known exactly but found only from numerical simulations [30]. The exponent  $1/2$  could be understood as follows. In  $d \geq 6$  the space restriction becomes irrelevant and the shortest path behaves like a random walk ( $\langle r^2 \rangle \sim t$  (time  $t$  is equivalent to  $l$ , i.e., the number of steps)). To derive Eq. (5) from a single scaling function, we propose the function,

$$\langle r \rangle = \zeta l^{1/2} f\left(\frac{l}{l^*}\right) \quad (6)$$

where,

$$f(x) = \begin{cases} const & x \leq 1 \\ x^{\phi_1} & x > 1 \end{cases} \quad (7)$$

Here,  $l^*$  is assumed to scale as  $\zeta^{d_{min}}$ . Indeed, from the scaling function Eq. (6), by using Eq. (7) and identifying  $\phi_1 \simeq 1/d_{min} - 1/2 \simeq 0.385$ , follows Eq. (5). Our scaling assumption Eq. (6) is supported by simulations shown in Fig. 2(b).

Next, we ask if the bi-universality phenomena found for the SNM is unique for percolation at criticality or whether it can also be observed far from criticality. Hence, we calculate directly both (i) the geometric distance as a function of chemical distance and (ii) the

network dimension when the network is full i.e., for  $p = 1$ . In both quantities we find that the SNM shows bi-universality phenomena. The algorithm to measure the geometric distance  $r$  as a function of chemical distance when the network is full is the same as described above for criticality. The only difference is that one should apply the algorithm when the network is full ( $p = 1$ ) and not at criticality. Simulation results are shown in Fig. 3(a). It is seen that for small  $l$  the distance  $r$  behaves approximately as  $r \sim l^{1/2}$  while for large  $l$ ,  $r \sim l$ . Indeed, we expect that the behavior of the network will follow:

$$\langle r \rangle = \begin{cases} l^{1/2} & l \leq l^{**} \\ l & l > l^{**}, \end{cases} \quad (8)$$

because at short distances ( $r < \zeta$ ) we expect a random behavior and at large distances ( $r > \zeta$ ) a spatial behavior. Moreover, we expect  $l^{**}$  to scale as  $\log \zeta$ . This is because in random networks the chemical distance  $l$  scales as  $\log N$  [20, 31] where  $N$  is the number of nodes within a chemical distance  $\leq l$  from a given node. On the other hand,  $N$  of the MF region scales as  $\zeta^2$ . Thus,  $l^{**}$  scales as  $\log \zeta$  as supported by simulations shown in Fig. 4 in the supplementary material. To derive Eq. (8) from a single scaling function, we propose the scaling function,

$$\langle r \rangle = l^{1/2} f\left(\frac{l}{l^{**}}\right) \quad (9)$$

where,

$$f(x) = \begin{cases} const & x \leq 1 \\ x^{1/2} & x > 1 \end{cases} \quad (10)$$

Our assumption, Eq. (10), is supported by simulations as shown in Fig. 3(a). Note that Fig. 3(a) is based on the scaling function in Eq. (9) and Eq. (10). In this figure, the graph starts as a constant and then a crossover emerges and the exponent approaches  $1/2$ . As can be seen, as  $\zeta$  increases the crossover emerges at larger  $l$ . Note that for pure lattice there is no constant range behavior at all. Fig. 4 in the supplementary material demonstrates that indeed the scaling of  $l^{**}$  with  $\zeta$  follows  $\log \zeta$ , as predicted by our approach. Both, Fig. 3(a) and Fig. 4 in the supplementary material support Eqs. (9) and (10).

We also evaluated directly the network dimensionality at  $p = 1$ . For this we first measure  $\langle r \rangle$  as a function of  $l$  as can be seen in Fig. 3(a), and then we calculated the mass,  $M$ , as function of  $l$ . Using both measurements we can plot in a double logarithmic plot  $M$  vs  $r$  whose slope (exponent) determines the dimension  $d$  of the system [4]. The results are demonstrated in Fig. 3(b), where the slope (power law exponent) represents the network dimensionality. At short scales the slope approaches infinity i.e., the dimensionality tends to infinity and at large scales the slope approaches 2 indicating that the dimensionality of the network is 2 as expected for 2d spatial

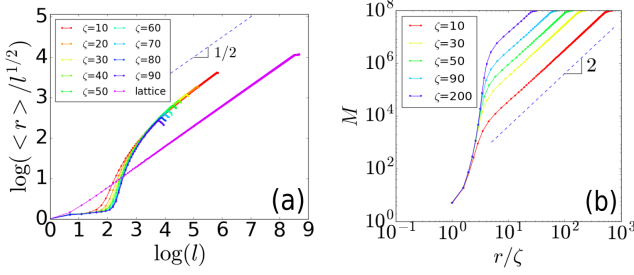


FIG. 3: (a) The average geometric distance  $\langle r \rangle$  as a function of the chemical distance  $l$  when the network is full ( $p = 1$ ). The scaling relation shown:  $r = l^{1/2} f(x)$ . It can be seen that after scaling the graph behavior starts approximately as a constant and then crosses over to exponent of  $1/2$ . For lattice the constant region does not exist and as  $\zeta$  increases the constant region gets longer. The scaling of the crossover point  $l^{**}$  with  $\zeta$  is shown in Fig. 4 in the supplementary material. (b) The dimension of the system when the network is at  $p = 1$ . It can be seen that at short scales the slope of the graph is diverging representing  $d = \infty$  as can be also seen in Fig. 7 in the supplementary material. For large  $r$  a crossover emerges and the graph changes its behavior as in spatial 2d system with a slope of 2. Simulations shown for  $N = 10^8$ , average over 200 realizations.

network. Note, as  $\zeta$  increases, the crossover emerges at larger  $l$  and the slope of the mean-field region tends to infinite as can be seen in Fig. 7 in the supplementary material.

Finally, we ask if the bi-universality phenomena also appears in a dynamical process on the network. To this end, we analyze the epidemic spread of the SIR model with a recovery time  $\tau = 1$  [32]. We measured the probability of the disease to stay alive at time  $t$  at criticality (i.e.  $p = p_c$ ). The parameter  $p$  represents the infection probability. The expected critical exponents for MF and lattice are as follows: (i) For the MF case: once a node is infected, the distribution of the sizes  $s$  of infected clusters is  $n(s) \sim s^{-3/2}$  and  $s \sim l^2$  [5]. Here  $l$  is the chemical distance which represents the time of infection. Hence, the distribution of infection times,  $l$ , is

$$p(l) \sim n(s) \frac{ds}{dl} \sim s^{-3/2} \cdot l = l^{-2}.$$

Thus, the probability that the epidemic will survive at time  $t = l$  scales as,  $\int p(l) dl \sim l^{-1}$ .

(ii) For the lattice case:  $n(s) \sim s^{-\tau+1}$ , where  $\tau = 1 + d/d_f$  and  $s \sim l^{d_{min}}/d_f$  [5]. Hence,

$$p(l) \sim n(s) \frac{ds}{dl} \sim s^{-d/d_f} \cdot l^{\frac{d_f}{d_{min}}-1} \sim l^{-(d-d_f)/d_{min}-1}.$$

For the lattice case it is known [5, 10] that  $d_f = 91/48$  and  $d_{min} = 1.13$ , therefore,  $\int p(l) dl \sim l^{-0.092}$ . Thus, we expect that the probability of the disease to stay alive at

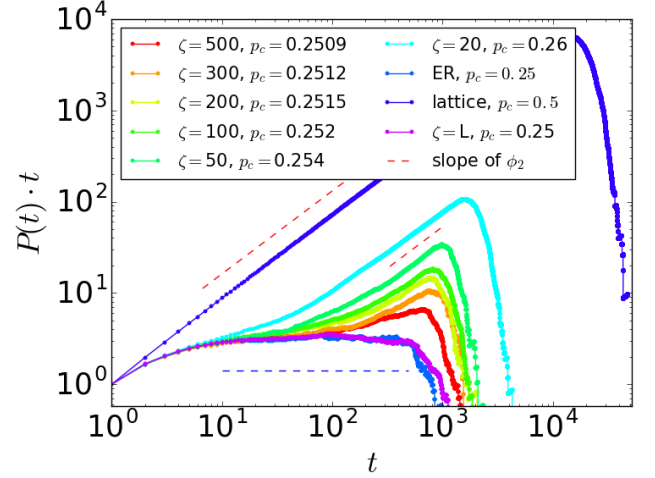


FIG. 4: The probability for the epidemic to be alive at time  $t$  on the SIR model. Scaled according to Eq. (12). The SIR model is simulated by infection of nearest neighbors bonds, with probability  $p$ . The scaling relation is :  $P(t) = t^{-1} f\left(\frac{t}{t^*}\right)$ . Each value of  $\zeta$  has a unique critical value for  $p_c$ . It can be seen that after scaling the graph behavior starts similar to mean field behavior and then a crossover emerges to a slope with exponent  $\phi_2$  as expected from spatial behavior. Note that for the lattice case there is no constant region at all. Simulations shown for  $N = 5000 \times 5000$ , average over 5000 realizations.

time  $t$  to follow:

$$P(t) = \begin{cases} t^{-1} & t \leq t^* \quad (MF) \\ t^{-0.092} & t > t^* \quad (lattice). \end{cases} \quad (11)$$

To derive Eq. (11) from a single scaling function, we propose the function,

$$P(t) = t^{-1} f\left(\frac{t}{t^*}\right) \quad (12)$$

where  $t^* \sim \zeta^{d_{min}}$  and

$$f(x) = \begin{cases} const & x \leq 1 \\ x^{\phi_2} & x > 1 \end{cases}. \quad (13)$$

After scaling using both Eq. (12) and Eq. (13) we get  $\phi_2 \simeq 1 - 0.092 \simeq 0.908$ . Indeed, simulations of SIR epidemic model are shown in Fig. 4 to scale according to Eq. (12). In this figure, the graph starts with MF behavior and then a crossover emerges and the exponent approaches  $\phi_2$ . Thus, supporting the bi-universality also for an epidemic process in such networks. As can be seen, as  $\zeta$  increases the crossover emerges at larger  $t$ . Note that for pure lattice there is no constant region at all. We also measured the infected mass as a function of time, presented in Fig. 4 of the Supplementary material.

To determine  $p_c$  for each  $\zeta$  we measured the infected mass for different values of  $p$ . For  $p > p_c$  the slope of the

graph is increasing, for  $p < p_c$  the slope is decaying and only for  $p = p_c$  the slope is stabilized at a specific value. Also, at  $p_c$  the time of epidemics is the longest. Simulations of this measurement are demonstrated in Fig. 6 in the Supplementary material.

In summary, we show that the realistic SNM developed here is represented by two critical regions caused by the exponential distribution of link lengths, Eq. (1), embedded in 2d. We expect that this finding to be general and also other physical phenomena such as polymers, Ising magnetic systems and diffusion on networks with exponential link-length distribution will present same phenomena of bi-universality represented by two sets of critical exponents. This bi-universality finding sheds

---

light on processes such as epidemic spreading in real world networks. For example, it shows that epidemics within cities (where it is easy to get everywhere) have a different laws compared to epidemic between cities.

We acknowledge the financial support of ONR Grant, N62909-16-1-2170; the DTRA Grant: HDTRA-1-10-1-0014 and HDTRA-1-09-1-0035, the BSF-NSF No. 2015781; the European MULTIPLEX Project, the Israel Ministry of Science and Technology with the Italy Ministry of Foreign Affairs; and MOST with the Japan Science and Technology Agency. MMD thanks the Azrieli Foundation for the award of an Azrieli Fellowship grant.

## Supplementary Information

### A. Degree Distribution and Link Length Distribution

We measured the degree distribution and the link length distribution as shown in Fig. 5 and Fig. 6 respectively. The degree distribution follows a Poisson distribution and the link length distribution follows  $P(r) \sim \exp(-r/\zeta)$  as expected in our model.

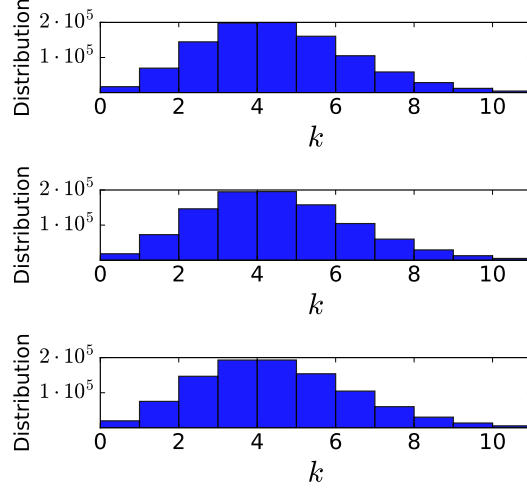


FIG. 5: **Degree distribution.** Histogram for the number of nodes with degree  $k$  shown for different values of  $\zeta$ . Top panel for  $\zeta = 5$ , middle panel for  $\zeta = 10$  and the lower panel for  $\zeta = 30$ . It can be seen that for all  $\zeta$ , the degree distribution follows Poisson distribution. The system has  $10^6$  nodes and  $\langle k \rangle = 4$ .

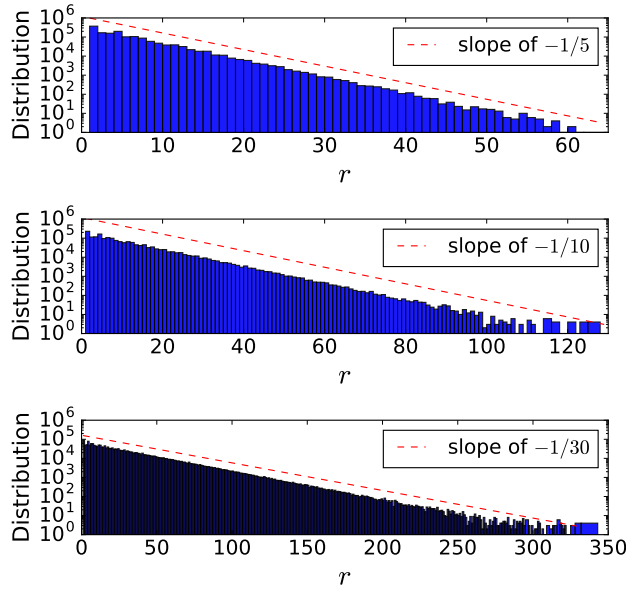


FIG. 6: **Link length distribution.** Histogram for the number of links with length  $r$  shown for different values of  $\zeta$  on a semi-log scale. Top panel for  $\zeta = 5$ , middle panel for  $\zeta = 10$  and the lower panel for  $\zeta = 30$ . It can be seen that the link length distribution follows the relation:  $P(r) \sim \exp(-r/\zeta)$ . The system has  $10^6$  nodes and  $\langle k \rangle = 4$ .

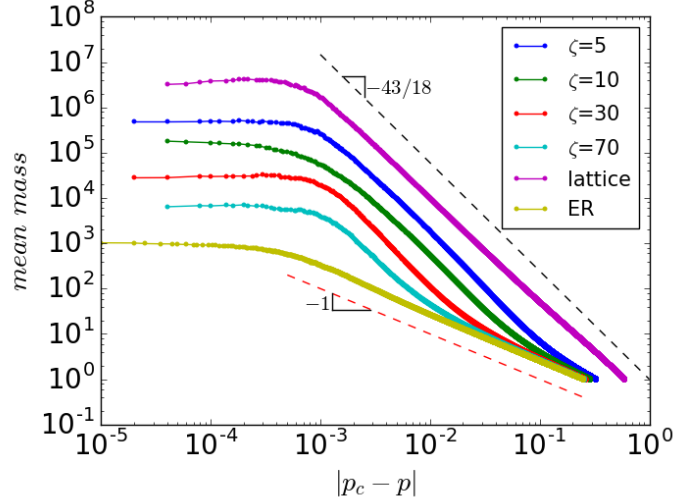


FIG. 7: **The mean mass as a function of  $|p_c - p|$  below criticality.** The network size is  $N = 10^4 \times 10^4$  nodes. Averages are taken over more than 200 realizations. It is seen that the two critical exponents coexist,  $\gamma_{lattice} = 43/18$  for large distances and  $\gamma_{MF} = 1$  for short distances. The crossover emerges closer to criticality as  $\zeta$  increases.

### B. The critical exponent $\gamma$

We also measured the mean mass of all the clusters except the infinite cluster as function of  $|p - p_c|$  near  $p_c$ ,

$$\langle S \rangle = \frac{1}{N} \sum s_i^2 n_i \quad (B1)$$

where  $s_i$  is the cluster size,  $n_i$  is the number of clusters of size  $s_i$  and  $N$  is the number of the active nodes in the network.

As can be seen in Fig. 7, two values for the critical exponent  $\gamma$ , the exponent of the mean mass, coexist. At large scales, close to criticality, the mean mass demonstrates scaling behavior with  $\gamma \approx 43/18$ . At short scales (further from  $p_c$ ) the mean mass demonstrates scaling behavior with  $\gamma \approx 1$ . As  $\zeta$  increases the crossover emerges closer to criticality. The values of the critical exponent  $\gamma$  have already been calculated for lattice and mean field respectively to be  $\gamma_{lattice} = 43/18$  and  $\gamma_{MF} = 1$  [5, 10]. As shown in the main manuscript for  $\nu$  and  $\beta$ ,  $\gamma$  takes the values according to the scaling behavior of the region and generally follows the relation:

$$\langle S \rangle \sim |p - p_c|^{-\gamma} \quad \text{where} \quad \begin{cases} \gamma = 1 & p < p^* \\ \gamma = 43/18 & p_c > p > p^* \end{cases} \quad (B2)$$

when  $p$  approaches  $p_c$ . The parameter  $p$  represents the probability for a single node to be active (not removed) in the network and  $p^*$  represents the crossover point.

### C. The crossover point $l^{**}$

In Fig. 8 we show the crossover point  $l^{**}$  between the two regions for the measurement shown in Fig. 3(a) in the main manuscript. It can be seen the  $l^{**}$  scales as  $\log \zeta$ .

### D. Infected mass as function of time

To further analyze the epidemic process, we also measured the number of infected nodes,  $s$ , at time  $t$ . The expected behavior of  $s$  in the two different regions are as follow:

(i) For the MF case:  $s \sim t^2$  and the expected value of the mass infected at step  $l = t$ , is the derivative of  $s$ , hence, the expected slope is 1.



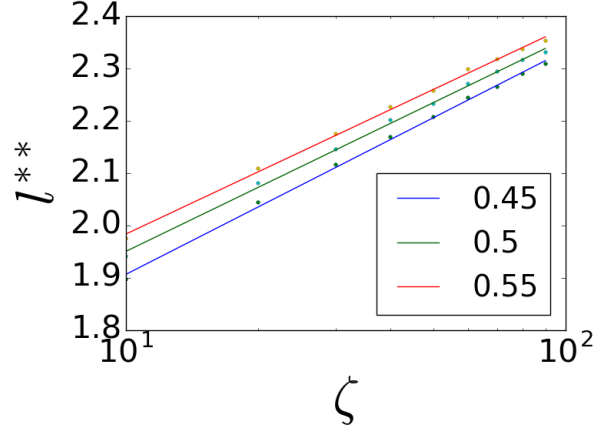


FIG. 8: **The crossover point  $l^{**}$  as a function of  $\zeta$ .** Obtained for different values of  $\log(\langle r \rangle / l^{1/2})$  just above the constant region.

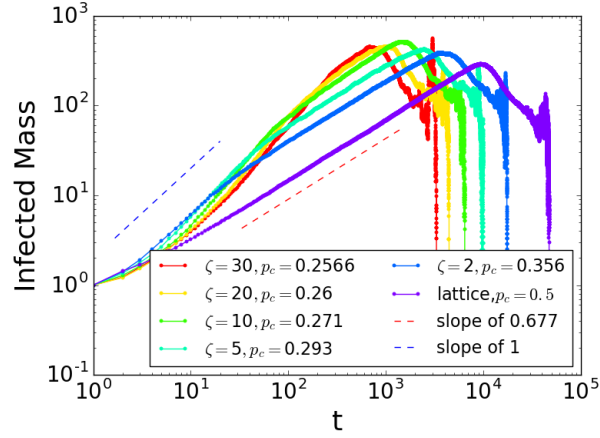


FIG. 9: **The infected mass at time  $t$ .** Averages are taken over more then 5000 realizations where each network has  $5000 \times 5000$  nodes. Each value of  $\zeta$  has a unique critical value for  $p_c$  found by the method described in the text. It can be seen that the graph starts with MF behavior and then crossover to spatial behavior. Note that for the lattice there is no MF behavior and as  $\zeta$  increases the crossover emerges at larger  $t$ .

(ii) For the SL case:  $s \sim l^{\frac{d_f}{d_{min}}}$  and the expected value is the derivative of  $s$ , hence, the expected slope is  $l^{\frac{d_f}{d_{min}}-1} \sim l^{0.677}$ .

Simulations of the infected mass at time  $t$  is shown in Fig. 9. As can be seen, the graph starts with MF behavior (slope 1) and then crossover to spatial behavior (slope 0.677). Note that for the lattice there is no MF behavior region at all and as  $\zeta$  increases the crossover emerges at larger  $t$ .

### E. The critical value for the infection probability $p$

To determine  $p_c$  for epidemics with the SIR model we measured for each  $\zeta$ , the spreading for different values for  $p$ . It can be seen in Fig. 10 for  $\zeta = 5$ , that for  $p > p_c$  the slope is increasing with time  $t$ , for  $p < p_c$  the slope is decaying and for  $p = p_c$  the slope stabilized on the expected slope which matches that of spatial region. Note that the spreading time for  $p_c$  is the longest as can be seen in the figure.



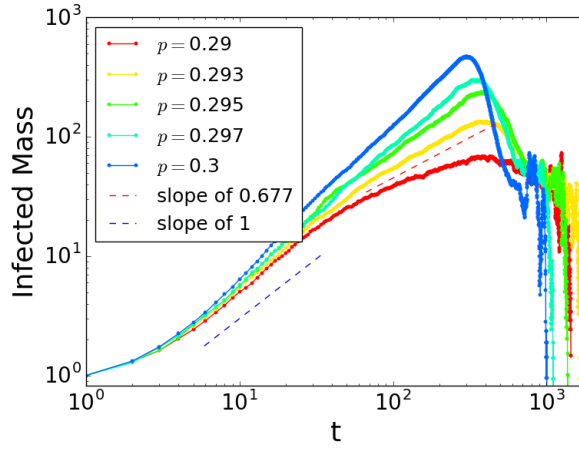


FIG. 10: **Infected mass as function of time for  $\zeta = 5$  for SIR model.** The network size is  $N = 2000 \times 2000$  nodes. Averages are taken over more than 5000 realizations. It can be seen that for  $p > p_c = 0.293$  the slope is increasing, for  $p < p_c$  the slope is decaying while for  $p = p_c = 0.293$  the slope stabilized on the expected slope of the spatial region. Note that the spreading time for  $p_c$  is also the longest as can be seen in the figure.

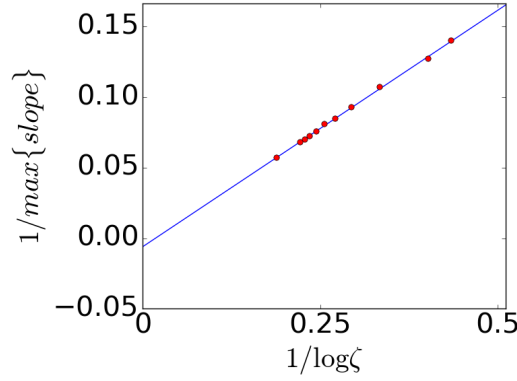


FIG. 11: **The maximal slope of the network dimension as function of  $\zeta$ .** It can be seen that as  $\zeta$  increases the maximal slope tends to infinity.

#### F. The maximum slope of the network dimension

In Fig. 11 we show the maximal slope of the network dimension as been shown in Fig. 3(b) in the main manuscript. This figure shows clearly that at short scales the slope of the graph is diverging representing  $d = \infty$ .

- 
- [1] K. Huang, *Introduction to statistical physics* (CRC Press, 2009).
  - [2] R. J. Baxter, *Exactly solved models in statistical mechanics* (Courier Corporation, 2007).
  - [3] H. Stanley, *Introduction to Phase Transitions and Critical Phenomena*, International series of monographs on physics (Oxford University Press, 1971).
  - [4] D. Li, K. Kosmidis, A. Bunde, and S. Havlin, *Nature Physics* **7**, 481 (2011).
  - [5] A. Bunde and S. Havlin, *Fractals and disordered systems* (Springer-Verlag New York, Inc., 1991).
  - [6] G. Mussardo, *Statistical field theory: an introduction to exactly solved models in statistical physics* (Oxford University Press, 2010).
  - [7] A. Coniglio, *Physical review letters* **62**, 3054 (1989).
  - [8] P.-G. De Gennes, *Scaling concepts in polymer physics* (Cornell university press, 1979).
  - [9] S. Kirkpatrick, *Rev. Mod. Phys.* **45**, 574 (1973).
  - [10] D. Stauffer and A. Aharony, *Introduction to Percolation Theory* (Taylor & Francis, 1994).

- [11] A. Coniglio, Journal of Physics A: Mathematical and General **15**, 3829 (1982).
- [12] J. S. Andrade Jr, H. J. Herrmann, R. F. Andrade, and L. R. Da Silva, Physical Review Letters **94**, 018702 (2005).
- [13] M. M. Danziger, L. M. Shekhtman, Y. Berezin, and S. Havlin, EPL (Europhysics Letters) **115**, 36002 (2016).
- [14] S. Soltan and G. Zussman, in *Power and Energy Society General Meeting (PESGM), 2016* (IEEE, 2016) pp. 1–5.
- [15] E. Bullmore and O. Sporns, Nature Reviews Neuroscience **13**, 336 (2012).
- [16] M. Kaiser, NeuroImage **57**, 892 (2011).
- [17] M. Barthélemy, Physics Reports **499**, 1 (2011).
- [18] W. Li *et al.*, Phys. Rev. Lett. **108**, 228702 (2012).
- [19] B. Bollobás, *Random Graphs*, 2nd ed. (Cambridge University Press, 2001).
- [20] M. Newman, *Networks: an introduction* (OUP Oxford, 2010).
- [21] D. J. Watts and S. H. Strogatz, Nature **393**, 440 (1998).
- [22] M. Barthélemy and L. A. N. Amaral, Physical Review Letters **82**, 3180 (1999).
- [23] M. T. Gastner and M. E. Newman, The European Physical Journal B-Condensed Matter and Complex Systems **49**, 247 (2006).
- [24] S. N. Dorogovtsev, A. V. Goltsev, and J. F. F. Mendes, Rev. Mod. Phys. **80**, 1275 (2008).
- [25] Schneider *et al.*, Proceedings of the National Academy of Sciences **108**, 3838 (2011).
- [26] A. Halu, S. Mukherjee, and G. Bianconi, Phys. Rev. E **89**, 012806 (2014).
- [27] S. Bradde, F. Caccioli, L. Dall’Asta, and G. Bianconi, Phys. Rev. Lett. **104**, 218701 (2010).
- [28] B. Waxman, Selected Areas in Communications, IEEE Journal on **6**, 1617 (1988).
- [29] M. M. Danziger, S. V. Buldyrev, B. Gross, and S. Havlin, (to be published) (2017).
- [30] H. J. Herrmann and H. E. Stanley, Journal of Physics A: Mathematical and General **21**, L829 (1988).
- [31] R. Cohen and S. Havlin, *Complex Networks: Structure, Robustness and Function* (Cambridge University Press, 2010).
- [32] A. Barrat, M. Barthelemy, and A. Vespignani, *Dynamical processes on complex networks* (Cambridge university press, 2008).